

Oxygen Isotope Exchange Between Dust Aggregates and Ambient Nebular Gas

SOTA ARAKAWA ¹, DAIKI YAMAMOTO ², LILY ISHIZAKI ³, TAMAMI OKAMOTO ⁴, AND NORIYUKI KAWASAKI ⁵

¹*Center for Mathematical Science and Advanced Technology, Japan Agency for Marine-Earth Science and Technology, 3173-25 Showa-machi, Kanazawa-ku, Yokohama 236-0001, Japan*

²*Department of Earth and Planetary Sciences, Kyushu University, 744 Motoooka, Nishi-ku, Fukuoka 819-0395, Japan*

³*Department of Earth and Planetary Science, The University of Tokyo, 7-3-1 Hongo, Bunkyo-ku, Tokyo 113-0033, Japan*

⁴*Earth-Life Science Institute, Tokyo Institute of Technology, 2-12-1 Ookayama, Meguro-ku, Tokyo 152-8550, Japan*

⁵*Department of Earth and Planetary Sciences, Faculty of Science, Hokkaido University, Kita-10 Nishi-8, Kita-ku, Sapporo 060-0810, Japan*

ABSTRACT

Meteorites and their components exhibit a diverse range of oxygen isotope compositions, and the isotopic exchange timescale between dust grains and ambient gas is a key parameter for understanding the spatiotemporal evolution of the solar nebula. As dust grains existed as macroscopic aggregates in the solar nebula, it is necessary to consider the isotopic exchange timescales for these aggregates. Here, we theoretically estimate the isotope exchange timescales between dust aggregates and ambient vapor. The isotope exchange process between aggregates and ambient vapor is divided into four processes: (i) supply of gas molecules to the aggregate surface, (ii) diffusion of molecules within the aggregate, (iii) isotope exchange on the surface of constituent particles, and (iv) isotope diffusion within the particles. We evaluate these timescales and assess which one becomes the rate-determining step. We reveal that the isotope exchange timescale is approximately the same as that of the constituent particles when the aggregate radius is smaller than the critical value, which is a few centimeters when considering the exchange reaction between amorphous forsterite aggregates and water vapor.

Keywords: Astrochemistry (75) — Cosmochemistry (331) — Meteorites (1038) — Protoplanetary disks (1300)

1. INTRODUCTION

Oxygen is the most fundamental element for solids in the universe. Clayton et al. (1973) discovered a large oxygen isotopic anomaly in refractory inclusions of the Allende carbonaceous chondrite, and oxygen isotopic compositions of extraterrestrial materials have been intensively investigated in the fields of meteoritics and planetary science (e.g., Nakamura et al. 2008; Kawasaki et al. 2022; Lauretta et al. 2024).

Meteorites and their components exhibit a diverse range of oxygen isotope compositions (e.g., Schrader et al. 2013; Kawasaki et al. 2017; Marrocchi et al. 2018). This isotopic variation is usually interpreted as the result of mixing between isotopically distinct reservoirs in the solar nebula (e.g., Ushikubo et al. 2012; Kawasaki et al. 2018; Tenner et al. 2018; Yamamoto et al. 2022). The reservoirs would be formed through self-shielding of carbon monoxide (CO) gas in the protosolar molecular cloud (e.g., Yurimoto & Kuramoto 2004; Krot et al. 2020) or the early solar nebula (e.g., Lyons & Young 2005). Minor CO isotopologues (i.e., C¹⁷O and C¹⁸O) are selectively dissociated by irradiation

of ultraviolet photons and ¹⁶O-poor oxygen atoms are produced. They are subsequently transformed into ¹⁶O-poor water (H₂O) ice through chemical reactions at the surface of dust grains (e.g., Yurimoto & Kuramoto 2004). Considering the mass balance, the residual CO gas would be enriched in ¹⁶O. As a result, the three major oxygen reservoirs (i.e., H₂O, CO, and silicate) would have distinct isotope compositions (e.g., Furuya et al. 2022; Nomura et al. 2023). The material evidence for the presence of ¹⁶O-poor H₂O reservoir in the solar nebula is preserved as cometary H₂O ice (e.g., Altwegg et al. 2019) and ¹⁶O-poor magnetite, formed by oxidation by H₂O, in “cosmic symplectite” found in the most primitive carbonaceous chondrite Acfer 094 (e.g., Sakamoto et al. 2007).

In a protoplanetary disk, dust grains drift radially due to gas drag and turbulent diffusion, and water ice sublimation occurs around the H₂O snowline (e.g., Okamoto & Ida 2022). Inward migration of icy dust grains could cause local enhancement of ¹⁶O-depleted H₂O relative to ¹⁶O-enriched CO (e.g., Cuzzi & Zahnle 2004; Krot et al. 2005). Both H₂O and CO vapors could react with silicate grains in the inner region of the disk where the temperature is high (e.g., Yamamoto et al. 2018, 2020, 2024; Ishizaki et al. 2023), leading to depletion/enrichment of silicate grains in ¹⁶O. Evaporation of silicate grains followed by recondensation also alters their

oxygen isotopic composition (e.g., Alexander 2004; Naga-hara & Ozawa 2012).

McKeegan et al. (2011) reported the oxygen isotopic composition of the Sun, which represents the average isotopic composition of the solar system. They found that the vast majority of silicate grains in the inner solar system were depleted in ^{16}O compared to the composition of the Sun. Assuming that silicate grains initially have a Sun-like isotope composition on average, the oxygen isotopic composition of silicate grains must evolve before the accretion of planetesimals. The isotopic exchange between pristine silicate dust components with the Sun-like oxygen isotopic compositions and ^{16}O -depleted H_2O vapor is a key process for the oxygen isotopic evolution in the solar nebula.

Dust grains in the interstellar medium are largely amorphous (e.g., Kemper et al. 2004). In contrast, astronomical observations at infrared wavelengths have revealed that both crystalline and amorphous silicate grains exist in protoplanetary disks, with forsterite being one of the most abundant crystalline silicate (e.g., Olofsson et al. 2009; Juhász et al. 2010). Therefore, we expect that amorphous forsterite represents the dust that existed in the early phase of the solar nebula.

The isotopic exchange timescale between dust grains and ambient gas is the key parameter to understanding the spatiotemporal evolution of oxygen isotopic composition of the solar nebula. Therefore, laboratory experiments of oxygen isotope exchange reaction under the disk-like low vapor pressure conditions are essential. In this context, Yamamoto et al. (2018) performed experiments of oxygen isotope exchange reaction between amorphous forsterite grains and water vapor and determined the isotopic exchange timescale. The timescales for different minerals and gases have also been investigated (e.g., Yamamoto et al. 2020, 2024). They found that, for amorphous forsterite grains with a radius of 1 micron or smaller, the timescale for oxygen isotope exchange at temperatures above approximately 600 K would be shorter than the lifetime of the solar nebula. Additionally, at temperatures below 800 K, isotope exchange occurs faster than forsterite crystallization.

However, dust grains exist as aggregates in protoplanetary disks (e.g., Tazaki et al. 2023) and the solar nebula (e.g., Bentley et al. 2016), necessitating consideration of aggregates' isotopic exchange timescales in discussions on the evolution of oxygen isotope compositions in the solar nebula. To quantify the effect of aggregate structure on the isotopic exchange timescale, understanding of the diffusion of gas molecules within the aggregate through its voids is essential. Recently, the diffusion of dilute gas within aggregates have been intensively investigated in the context of cometary science (e.g., Güttler et al. 2023; Skorov et al. 2024). We can employ theoretical models developed in the cometary science community for isotope exchange reaction of dust aggregates in the gaseous solar nebula. In addition, the surface-to-volume ratio decreases as dust grains grow into larger aggregates, potentially affecting the isotopic exchange timescale by controlling the supply of molecules at the surface of ag-

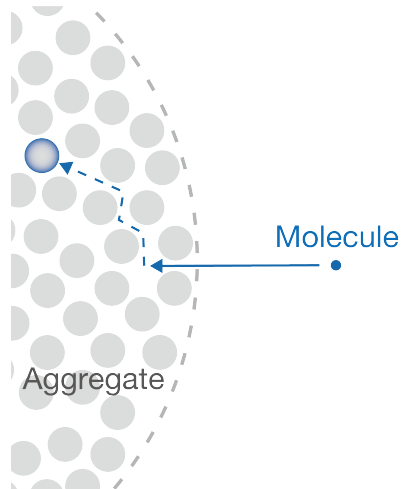


Figure 1. Schematic of the diffusion of gas molecules within a dust aggregate. First, molecules are supplied to the surface of the aggregate from the ambient gas. Some of these molecules are trapped within the aggregate, while others reflect off the aggregate surface without undergoing an exchange reaction. The trapped molecules then diffuse through the voids within the aggregate and react with the surface of the constituent particles. Finally, the isotopic composition of the constituent particles evolves through the diffusive exchange reaction within the particles.

gregates. We also quantify this effect and derive the critical aggregate radius below which the aggregate effects can be neglected.

In this study, we theoretically estimate the oxygen isotope exchange timescales between silicate dust aggregates and ambient water vapor. The isotope exchange process between aggregates and ambient vapor is divided into four processes (see Section 2). We evaluate the timescales of these processes and assess which one becomes the rate-determining step based on aggregate size, temperature, and water vapor pressure. Our analytical calculations reveal that, for dust aggregates smaller than cm size, the isotope exchange timescale is approximately the same as that of the constituent particles (see Section 3).

2. MODEL

Here, we construct a theoretical model of isotope exchange process between aggregates and ambient vapor. Figure 1 shows a schematic of gas molecule diffusion within a dust aggregate. The isotope exchange process between aggregates and ambient vapor is divided into four processes: (i) supply of gas molecules to the aggregate surface, (ii) diffusion of molecules within the aggregate, (iii) isotope exchange on the surface of constituent particles, and (iv) isotope diffusion within the particles. The timescales for these four processes are denoted as $t_{\text{agg,surf}}$, $t_{\text{agg,diff}}$, $t_{\text{par,surf}}$, and $t_{\text{par,diff}}$, respectively. We theoretically derive the equations for these four timescales and their parameter dependences in the following sections.

We evaluate the timescale for isotope exchange reaction, t_{ex} , as the sum of the timescales of the four processes:

$$t_{\text{ex}} = t_{\text{agg,surf}} + t_{\text{agg,diff}} + t_{\text{par,surf}} + t_{\text{par,diff}}. \quad (1)$$

The isotope exchange timescale for constituent particles is given by

$$t_{\text{ex,par}} = t_{\text{par,surf}} + t_{\text{par,diff}} \\ \approx \max(t_{\text{par,surf}}, t_{\text{par,diff}}). \quad (2)$$

Thus, the effect of aggregate structure on the isotopic exchange timescale is significant when the following condition is satisfied:

$$\max(t_{\text{agg,surf}}, t_{\text{agg,diff}}) \gtrsim t_{\text{ex,par}}. \quad (3)$$

2.1. Supply of Molecules at the Surface of Aggregates

For a spherical aggregate with a radius of r_{agg} , the timescale of the supply-controlled exchange reaction, $t_{\text{agg,surf}}$, is given by (e.g., Yamamoto et al. 2018)

$$t_{\text{agg,surf}} = \frac{N_{\text{agg}}}{\beta_{\text{agg}} J S_{\text{agg}}}, \quad (4)$$

where $S_{\text{agg}} = 4\pi r_{\text{agg}}^2$ is the surface area of the aggregate, N_{agg} is the number of oxygen atoms in the aggregate, β_{agg} is the exchange efficiency of molecules at the surface of the aggregate, and J is the supply flux of oxygen atoms. Here, J is given by

$$J = \frac{P\gamma_{\text{gas}}}{\sqrt{2\pi m k_{\text{B}} T}}, \quad (5)$$

where P is the partial pressure, m is the molecular weight, T is the temperature, and $k_{\text{B}} = 1.38 \times 10^{-23} \text{ J K}^{-1}$ is the Boltzmann constant. For water vapor, we set $m = 18m_{\text{H}}$, where $m_{\text{H}} = 1.67 \times 10^{-27} \text{ kg}$ is the mass of a hydrogen atom. We define the number of oxygen atoms per gas molecule as γ_{gas} , and $\gamma_{\text{gas}} = 1$ for H_2O .

The number of oxygen atoms in the aggregate, N_{agg} , is given by

$$N_{\text{agg}} = \frac{\phi_{\text{agg}} V_{\text{agg}} N_{\text{A}} \gamma_{\text{grain}}}{\Omega}, \quad (6)$$

where Ω is the molar volume of minerals, $V_{\text{agg}} = (4\pi/3)r_{\text{agg}}^3$ is the volume of the aggregate, ϕ_{agg} is the volume filling factor of the aggregate, and $N_{\text{A}} = 6.02 \times 10^{23} \text{ mol}^{-1}$ is the Avogadro constant. We set $\Omega = 50 \text{ cm}^3 \text{ mol}^{-1}$ for both amorphous and crystalline forsterite (Yamamoto et al. 2018). We define the number of oxygen atoms in the compositional formula of grains as γ_{grain} , and $\gamma_{\text{grain}} = 4$ for amorphous/crystalline forsterite (Mg_2SiO_4) grains.

The area fraction of holes on the surface of aggregates is equal to the porosity of aggregates, $1 - \phi_{\text{agg}}$. As exchange of molecules between aggregates and ambient gas occurs at the site of the hole on the surface of aggregates (see Figure 1), the exchange efficiency of molecules at the surface of the aggregate, β_{agg} , is approximately given by

$$\beta_{\text{agg}} = 1 - \phi_{\text{agg}}. \quad (7)$$

2.2. Diffusion of Molecules Within Aggregates

For a spherical aggregate with a radius of r_{agg} , the timescale of the diffusive exchange reaction, $t_{\text{agg,diff}}$, is given by (e.g., Crank 1979)

$$t_{\text{agg,diff}} = \frac{r_{\text{agg}}^2}{\pi^2 D_{\text{agg}}}, \quad (8)$$

where D_{agg} is the diffusion coefficient within an aggregate. For dust aggregates consisting of micron-sized grains, the size of voids is orders of magnitude smaller than the mean free path of gas molecules, and the random motion of gas molecules is governed by collisions with the particle surface (Knudsen 1909). In this situation, D_{agg} is given by (e.g., Derjaguin 1946; Güttler et al. 2023; Skorov et al. 2024)

$$D_{\text{agg}} = \frac{4r_{\text{par}}c_s(1 - \phi_{\text{agg}})^2}{13\phi_{\text{agg}}}, \quad (9)$$

where r_{par} is the radius of constituent particles and $c_s = \sqrt{(8k_{\text{B}}T)/(\pi m)}$ is the mean thermal velocity of molecules.

In Section 3, we show that $t_{\text{agg,diff}}$ for cm-sized aggregates is orders of magnitude shorter than the others ($t_{\text{agg,surf}}$, $t_{\text{par,surf}}$, and $t_{\text{par,diff}}$). Thus, the diffusion within aggregates is not the rate-limiting process.

2.3. Supply of Molecules at the Surface of Constituent Particles

For a spherical particle with a radius of r_{par} , the timescale of the supply-controlled exchange reaction, $t_{\text{par,surf}}$, is given by (e.g., Yamamoto et al. 2018)

$$t_{\text{par,surf}} = \frac{N_{\text{par}}}{\beta_{\text{par}} J S_{\text{par}}}, \quad (10)$$

where $S_{\text{par}} = 4\pi r_{\text{par}}^2$ is the surface area of the particle, $N_{\text{par}} = (V_{\text{par}} N_{\text{A}} \gamma_{\text{grain}})/\Omega$ is the number of oxygen atoms in the particle, and $V_{\text{par}} = (4\pi/3)r_{\text{par}}^3$ is the volume of the particle. The isotopic exchange efficiency of colliding molecules with particles, β_{par} , is determined from laboratory experiments. For amorphous forsterite grains reacting with water vapor, Yamamoto et al. (2018) measured the β_{par} value at $T \sim 800\text{--}900 \text{ K}$ and $P = 10^{-2} \text{ Pa}$. They found that

$$\beta_{\text{par}} = 7.4 \times 10^{-6}. \quad (11)$$

In this study, we neglect the temperature and pressure dependences of β_{par} for amorphous forsterite grains, although it would slightly depend on both T and P in reality (e.g., Yamamoto et al. 2024). We also assume that β_{par} for crystalline forsterite grains is the same as that for amorphous grains, although in reality, it might be significantly lower than what we assumed for simplicity.

2.4. Diffusion Within Constituent Particles

For a spherical particle with a radius of r_{par} , the timescale of the diffusive exchange reaction, $t_{\text{par,diff}}$, is given by (e.g., Crank 1979)

$$t_{\text{par,diff}} = \frac{r_{\text{par}}^2}{\pi^2 D_{\text{par}}}, \quad (12)$$

where D_{par} is the diffusive isotope exchange coefficient. The temperature dependence of D_{par} follows the Arrhenius law:

$$D_{\text{par}} = D_{\text{par,ref}} \exp \left[-\frac{E_a}{R_{\text{gas}}} \left(\frac{1}{T} - \frac{1}{T_{\text{ref}}} \right) \right], \quad (13)$$

where $R_{\text{gas}} = 8.31 \text{ J mol}^{-1} \text{ K}^{-1}$ is the gas constant, E_a is the activation energy, and $D_{\text{par,ref}}$ is the diffusive isotope exchange coefficient at the reference temperature, T_{ref} .

For amorphous forsterite grains in the ambient water vapor, Yamamoto et al. (2018) obtained the following values:

$$\begin{aligned} D_{\text{par,ref}} &= 1.5 \times 10^{-19} \text{ m}^2 \text{ s}^{-1}, \\ T_{\text{ref}} &= 1200 \text{ K}, \\ E_a &= 161.5 \text{ kJ mol}^{-1}. \end{aligned} \quad (14)$$

For crystalline forsterite grains, the temperature dependence of D_{par} is given by Equation (13) with the following constants¹ (Jaoul et al. 1980):

$$\begin{aligned} D_{\text{par,ref}} &= 3.6 \times 10^{-18} \text{ m}^2 \text{ s}^{-1}, \\ T_{\text{ref}} &= 1823 \text{ K}, \\ E_a &= 320 \text{ kJ mol}^{-1}. \end{aligned} \quad (15)$$

3. RESULTS & DISCUSSION

We calculate the timescale for oxygen isotope exchange between dust aggregates and ambient gas, t_{ex} , and investigate which process is the rate-limiting step. For simplicity, we assume that dust aggregates are made of monodisperse spherical particles with radius of $r_{\text{par}} = 0.1 \mu\text{m}$ (e.g., Tazaki et al. 2023). The volume filling factor of aggregates is set to $\phi_{\text{agg}} = 0.3$.² In this section, we consider oxygen isotope exchange with water vapor with partial pressure of $P = 10^{-4} \text{ Pa}$.

Figure 2 shows t_{ex} as a function of r_{agg} . Here, we assume that aggregates are made of amorphous forsterite grains. It is evident that $t_{\text{agg,surf}}$ is proportional to r_{agg} and $t_{\text{agg,diff}}$ is proportional to r_{agg}^2 (see Equations (4) and (8), respectively). In contrast, $t_{\text{par,surf}}$ and $t_{\text{par,diff}}$ are independent of r_{agg} . We also reveal that $t_{\text{agg,diff}}$ is orders of magnitude shorter than the other three timescales. In other words, diffusion of molecules within aggregates is not the rate-limiting step.

Both $t_{\text{par,diff}}$ and $t_{\text{par,surf}}$ depend on T , and $t_{\text{par,diff}} > t_{\text{par,surf}}$ when $T = 700 \text{ K}$ (see Figure 2(a)). In this case, either $t_{\text{par,diff}}$ or $t_{\text{agg,surf}}$ is the rate-limiting step: $t_{\text{ex}} \simeq t_{\text{par,diff}}$ when $r_{\text{agg}} < 24 \text{ cm}$, whereas $t_{\text{ex}} \simeq t_{\text{agg,surf}}$ when $r_{\text{agg}} > 24 \text{ cm}$. In contrast, for $T = 800 \text{ K}$ (see Figure 2(b)),

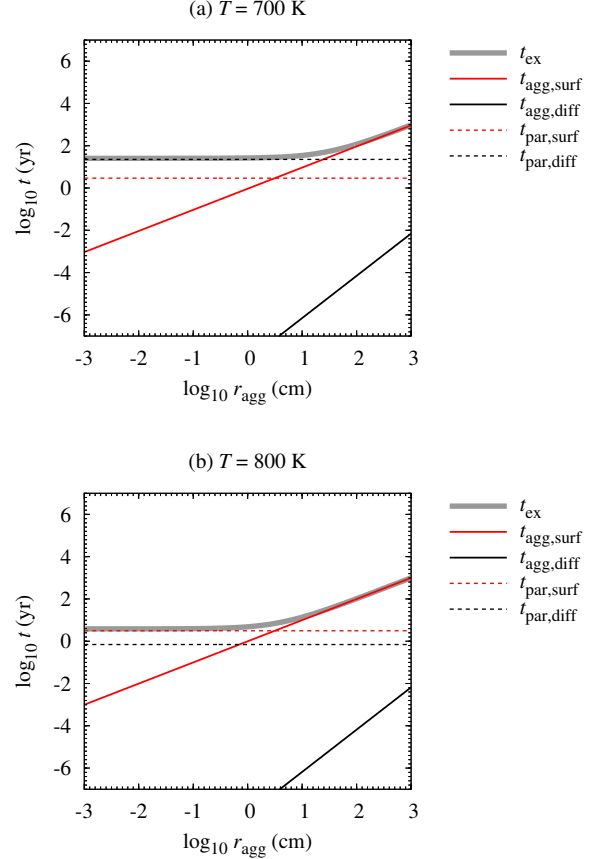


Figure 2. Timescale for oxygen isotope exchange between dust aggregates and ambient nebular gas, t_{ex} , as a function of aggregate radius, r_{agg} . (a) For $T = 700 \text{ K}$. (b) For $T = 800 \text{ K}$. Here, we assume that aggregates are made of amorphous forsterite grains. The timescales for four elementary processes ($t_{\text{agg,surf}}$, $t_{\text{agg,diff}}$, $t_{\text{par,surf}}$, and $t_{\text{par,diff}}$) are also plotted in the figure (see legends).

$t_{\text{par,surf}} > t_{\text{par,diff}}$, thus either $t_{\text{par,surf}}$ or $t_{\text{agg,surf}}$ is the rate-limiting step: $t_{\text{ex}} \simeq t_{\text{par,surf}}$ when $r_{\text{agg}} < 3.2 \text{ cm}$, whereas $t_{\text{ex}} \simeq t_{\text{agg,surf}}$ when $r_{\text{agg}} > 3.2 \text{ cm}$.

We also show the temperature dependence of t_{ex} in Figure 3. Here, we calculate t_{ex} for both amorphous and crystalline cases, and r_{agg} is set to 1 cm or 10 cm. Figure 3(a) shows the results for $r_{\text{agg}} = 1 \text{ cm}$ and aggregates are made of amorphous forsterite particles. We find that $t_{\text{ex}} \simeq t_{\text{par,diff}}$ when $T < 750 \text{ K}$, whereas $t_{\text{ex}} \simeq t_{\text{par,surf}}$ when $T > 750 \text{ K}$. In this case, $\max(t_{\text{agg,surf}}, t_{\text{agg,diff}})$ is smaller than $t_{\text{ex,par}}$ at an arbitrary temperature, and the impact of aggregate structure on the isotopic exchange timescale is negligible.

Amorphous silicate grains are crystallized under high temperature conditions by thermal annealing (e.g., Fabian et al. 2000). The timescale of crystallization, t_{cry} , is given by

$$t_{\text{cry}} = \frac{1}{\nu_0} \exp \left(\frac{E_{\text{cry}}}{R_{\text{gas}} T} \right), \quad (16)$$

¹ The mechanism for the diffusive isotope exchange within grains depends on whether the grains are amorphous or crystalline. It could also depend on the molecular species of the ambient vapor (see also Morizet et al. 2010; Kuroda et al. 2018, 2019; Yoshioka et al. 2019).

² The choice of $\phi_{\text{agg}} = 0.3$ is motivated from numerical simulations (e.g., Zsom et al. 2010; Arakawa et al. 2023) and laboratory experiments (e.g., Weidling et al. 2009; Kothe et al. 2013) on collisional growth of dust aggregates.

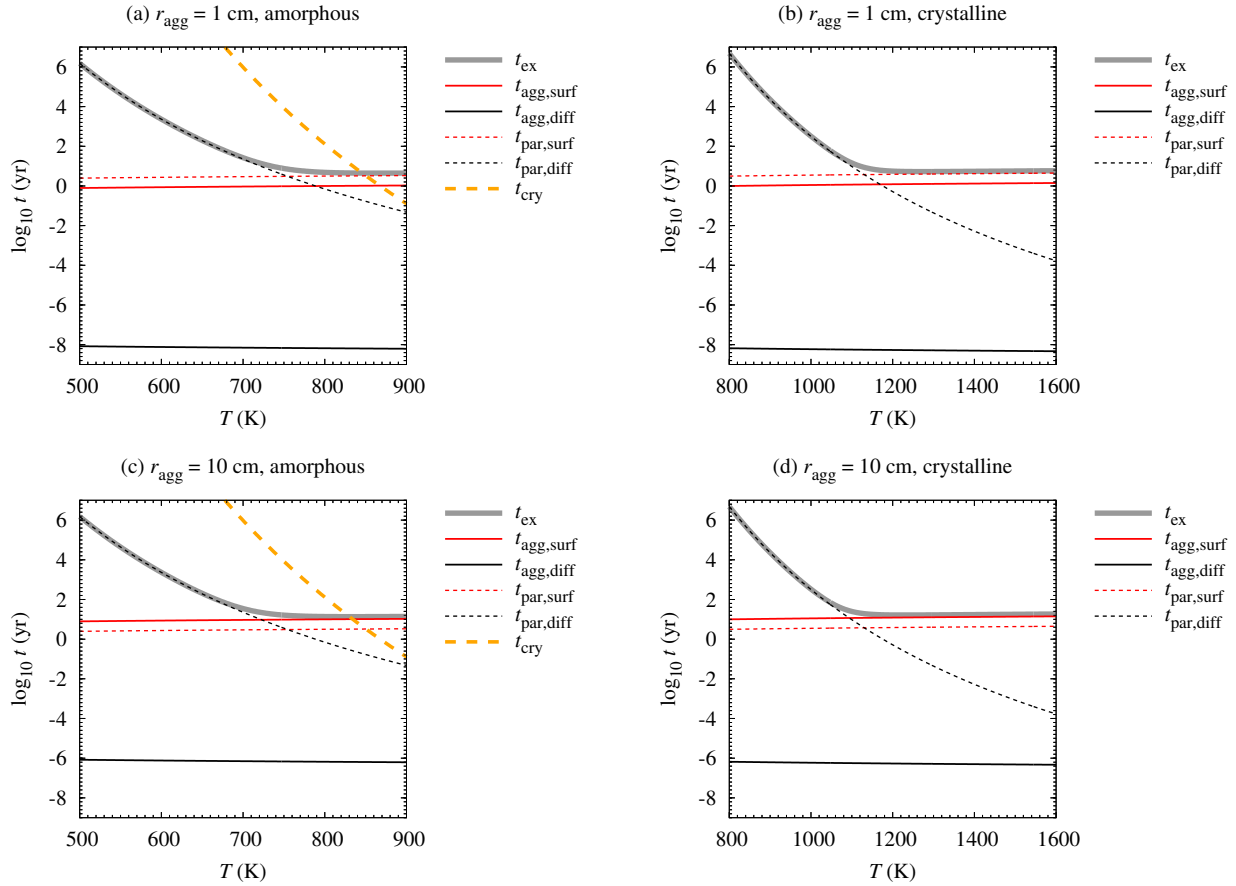


Figure 3. Timescale for oxygen isotope exchange between dust aggregates and ambient nebular gas, t_{ex} , as a function of temperature, T . (a) For $r_{\text{agg}} = 1$ cm and aggregates are made of amorphous forsterite particles. (b) For $r_{\text{agg}} = 1$ cm and aggregates are made of crystalline forsterite particles. (c) For $r_{\text{agg}} = 10$ cm and aggregates are made of amorphous forsterite particles. (d) For $r_{\text{agg}} = 10$ cm and aggregates are made of crystalline forsterite particles. The timescales for four elementary processes ($t_{\text{agg,surf}}$, $t_{\text{agg,diff}}$, $t_{\text{par,surf}}$, and $t_{\text{par,diff}}$) and for crystallization (t_{cry}) are also plotted in the figure (see legends).

where ν_0 is the pre-exponential factor of the crystallization rate and E_{cry} is the activation energy for crystallization. For amorphous forsterite grains with the ambient water vapor pressure of $P = 10^{-4}$ Pa, Yamamoto & Tachibana (2018) found that $\ln(\nu_0/1 \text{ Hz}) = 40.2$ and $E_{\text{cry}} = 414.4 \text{ kJ mol}^{-1}$. As shown in Figure 3(a), t_{cry} drastically decreases with increasing T , and $t_{\text{cry}} = 1 \text{ Myr}$ at $T = 700 \text{ K}$. Thus, a significant fraction of silicate dust particles in a high temperature region of $T > 700 \text{ K}$ would be crystallized within a lifetime of protoplanetary disk. The dynamics of dust aggregates also affect the crystallization temperature (see Ishizaki et al. 2023).

Figure 3(b) shows the temperature dependence of t_{ex} for the case of $r_{\text{agg}} = 1$ cm and aggregates are made of crystalline forsterite particles. As is the case for Figure 3(a), $\max(t_{\text{agg,surf}}, t_{\text{agg,diff}})$ is always smaller than $t_{\text{ex,par}}$, and t_{ex} is approximately given by $t_{\text{ex}} \approx t_{\text{ex,par}}$.

To understand the condition where the impact of aggregate structure on the isotopic exchange timescale becomes important, we compare $t_{\text{agg,surf}}$ with $t_{\text{par,surf}}$. The ratio of the two

timescales, $t_{\text{agg,surf}}/t_{\text{par,surf}}$, is given by

$$\begin{aligned} \frac{t_{\text{agg,surf}}}{t_{\text{par,surf}}} &= \frac{\beta_{\text{par}} \phi_{\text{agg}} r_{\text{agg}}}{(1 - \phi_{\text{agg}}) r_{\text{par}}} \\ &= 0.32 \left(\frac{\beta_{\text{par}}}{7.4 \times 10^{-6}} \right) \left(\frac{r_{\text{agg}}}{1 \text{ cm}} \right). \end{aligned} \quad (17)$$

Therefore, $t_{\text{agg,surf}}$ becomes larger than $t_{\text{par,surf}}$ when $r_{\text{agg}} > 3 \text{ cm}$. We validate this prediction in Figures 3(c) and 3(d). For $r_{\text{agg}} = 10 \text{ cm}$, $t_{\text{agg,surf}}$ is indeed larger than $t_{\text{par,surf}}$, and $t_{\text{agg,surf}}$ becomes the rate-limiting process at a high temperature ($T > 720 \text{ K}$ for the amorphous case and $T > 1090 \text{ K}$ for the crystalline case). We note that $t_{\text{agg,surf}}/t_{\text{par,surf}}$ is independent of Ω and γ_{grain} .

Multi-wavelength observations of protoplanetary disks at (sub)millimeter wavelengths allow us to constrain the size of dust aggregates and its radial distribution (e.g., Carrasco-González et al. 2019; Ueda et al. 2021). Several studies (e.g., Menu et al. 2014; Pérez et al. 2015; Tazzari et al. 2016) have reported that large aggregates with $r_{\text{agg}} \gtrsim 1 \text{ cm}$ are ubiquitous in the inner parts of disks where $r \lesssim 10 \text{ au}$, whereas the

maximum radius of aggregates is typically a few millimeters in the outer parts of $r \gtrsim 100$ au. Comets in the solar system also consist of millimeter- to decimeter-sized dust aggregates referred to as “pebbles” (e.g., Arakawa & Ohno 2020; Blum et al. 2022). These pieces of evidence support the presence of large dust aggregates in the ancient solar nebula.

In the protosolar molecular cloud, ^{16}O -poor H_2O reservoir would be formed through the self-shielding of CO gas, and silicates and volatiles have different oxygen isotopic compositions at the earliest stage of the solar nebula (e.g., Krot et al. 2020). Centimeter-sized icy dust aggregates drift toward the Sun due to gas drag (e.g., Adachi et al. 1976; Weidenschilling 1977), although the direction of radial migration depends on the sign of the pressure gradient (e.g., Arakawa et al. 2021). Furthermore, the radial migration of icy dust aggregates, followed by their evaporation at the snow line, could cause the spatiotemporal variation of oxygen isotopic composition in the gas component of the inner solar nebula (e.g., Cuzzi & Zahnle 2004; Krot et al. 2005).

In this study, we derived the fundamental equations for the isotope exchange process between aggregates and ambient vapor (Equations (4) and (8)). Using these equations, we

plan to investigate the spatiotemporal evolution of oxygen isotopic composition and silicate crystallinity, in conjunction with disk formation and evolution, in future studies.

4. CONCLUSION

In this study, we theoretically estimated the oxygen isotope exchange timescales between silicate dust aggregates and ambient water vapor. The isotope exchange process between aggregates and ambient vapor is divided into four processes (Section 2). We evaluated the timescales of these processes and assess which one becomes the rate-determining step. Our analytical calculations revealed that the isotope exchange timescale is approximately the same as that of the constituent particles when the aggregate radius is smaller than the critical value given by Equation (17) (Section 3). We plan to perform numerical simulations of oxygen isotopic evolution of the solar nebula using the theoretical model derived in this study.

ACKNOWLEDGMENTS

This work was supported by JSPS KAKENHI Grant Numbers JP24K17118 and JP21K13986.

REFERENCES

- Adachi, I., Hayashi, C., & Nakazawa, K. 1976, *Progress of Theoretical Physics*, 56, 1756, doi: [10.1143/PTP.56.1756](https://doi.org/10.1143/PTP.56.1756)
- Alexander, C. M. O. D. 2004, *GeoCoA*, 68, 3943, doi: [10.1016/j.gca.2004.03.030](https://doi.org/10.1016/j.gca.2004.03.030)
- Altwegg, K., Balsiger, H., & Fuselier, S. A. 2019, *ARA&A*, 57, 113, doi: [10.1146/annurev-astro-091918-104409](https://doi.org/10.1146/annurev-astro-091918-104409)
- Arakawa, S., Matsumoto, Y., & Honda, M. 2021, *ApJ*, 920, 27, doi: [10.3847/1538-4357/ac157e](https://doi.org/10.3847/1538-4357/ac157e)
- Arakawa, S., & Ohno, K. 2020, *MNRAS*, 497, 1166, doi: [10.1093/mnras/staa2031](https://doi.org/10.1093/mnras/staa2031)
- Arakawa, S., Okuzumi, S., Tatsuuma, M., et al. 2023, *ApJL*, 951, L16, doi: [10.3847/2041-8213/acdb5f](https://doi.org/10.3847/2041-8213/acdb5f)
- Bentley, M. S., Schmied, R., Mannel, T., et al. 2016, *Nature*, 537, 73, doi: [10.1038/nature19091](https://doi.org/10.1038/nature19091)
- Blum, J., Bischoff, D., & Gundlach, B. 2022, *Universe*, 8, 381, doi: [10.3390/universe8070381](https://doi.org/10.3390/universe8070381)
- Carrasco-González, C., Sierra, A., Flock, M., et al. 2019, *ApJ*, 883, 71, doi: [10.3847/1538-4357/ab3d33](https://doi.org/10.3847/1538-4357/ab3d33)
- Clayton, R. N., Grossman, L., & Mayeda, T. K. 1973, *Science*, 182, 485, doi: [10.1126/science.182.4111.485](https://doi.org/10.1126/science.182.4111.485)
- Crank, J. 1979, *The Mathematics of Diffusion* (Oxford University Press)
- Cuzzi, J. N., & Zahnle, K. J. 2004, *ApJ*, 614, 490, doi: [10.1086/423611](https://doi.org/10.1086/423611)
- Derjaguin, B. 1946, *CR Acad. Sci. URSS*, 53, 623
- Fabian, D., Jäger, C., Henning, T., Dorschner, J., & Mutschke, H. 2000, *A&A*, 364, 282
- Furuya, K., Tsukagoshi, T., Qi, C., et al. 2022, *ApJ*, 926, 148, doi: [10.3847/1538-4357/ac45ff](https://doi.org/10.3847/1538-4357/ac45ff)
- Güttler, C., Rose, M., Sierks, H., et al. 2023, *MNRAS*, 524, 6114, doi: [10.1093/mnras/stad2229](https://doi.org/10.1093/mnras/stad2229)
- Ishizaki, L., Tachibana, S., Okamoto, T., Yamamoto, D., & Ida, S. 2023, *ApJ*, 957, 47, doi: [10.3847/1538-4357/acf310](https://doi.org/10.3847/1538-4357/acf310)
- Jaoul, O., Froidevaux, C., Durham, W. B., & Michaut, M. 1980, *Earth and Planetary Science Letters*, 47, 391, doi: [10.1016/0012-821X\(80\)90026-6](https://doi.org/10.1016/0012-821X(80)90026-6)
- Juhász, A., Bouwman, J., Henning, T., et al. 2010, *ApJ*, 721, 431, doi: [10.1088/0004-637X/721/1/431](https://doi.org/10.1088/0004-637X/721/1/431)
- Kawasaki, N., Itoh, S., Sakamoto, N., & Yurimoto, H. 2017, *GeoCoA*, 201, 83, doi: [10.1016/j.gca.2015.12.031](https://doi.org/10.1016/j.gca.2015.12.031)
- Kawasaki, N., Simon, S. B., Grossman, L., Sakamoto, N., & Yurimoto, H. 2018, *GeoCoA*, 221, 318, doi: [10.1016/j.gca.2017.05.035](https://doi.org/10.1016/j.gca.2017.05.035)
- Kawasaki, N., Nagashima, K., Sakamoto, N., et al. 2022, *Science Advances*, 8, eade2067, doi: [10.1126/sciadv.ade2067](https://doi.org/10.1126/sciadv.ade2067)
- Kemper, F., Vriend, W. J., & Tielens, A. G. G. M. 2004, *ApJ*, 609, 826, doi: [10.1086/421339](https://doi.org/10.1086/421339)
- Knudsen, M. 1909, *Annalen der Physik*, 333, 75, doi: [10.1002/andp.19093330106](https://doi.org/10.1002/andp.19093330106)
- Kothe, S., Blum, J., Weidling, R., & Güttler, C. 2013, *Icarus*, 225, 75, doi: [10.1016/j.icarus.2013.02.034](https://doi.org/10.1016/j.icarus.2013.02.034)
- Krot, A. N., Nagashima, K., Lyons, J. R., Lee, J.-E., & Bizzarro, M. 2020, *Science Advances*, 6, eaay2724, doi: [10.1126/sciadv.aay2724](https://doi.org/10.1126/sciadv.aay2724)

- Krot, A. N., Hutcheon, I. D., Yurimoto, H., et al. 2005, *ApJ*, 622, 1333, doi: [10.1086/428382](https://doi.org/10.1086/428382)
- Kuroda, M., Tachibana, S., Sakamoto, N., et al. 2018, *American Mineralogist*, 103, 412, doi: [10.2138/am-2018-6208](https://doi.org/10.2138/am-2018-6208)
- Kuroda, M., Tachibana, S., Sakamoto, N., & Yurimoto, H. 2019, *American Mineralogist*, 104, 385, doi: [10.2138/am-2019-6802](https://doi.org/10.2138/am-2019-6802)
- Lauretta, D. S., Connolly, Harold C., J., Aebersold, J. E., et al. 2024, arXiv e-prints, arXiv:2404.12536, doi: [10.48550/arXiv.2404.12536](https://doi.org/10.48550/arXiv.2404.12536)
- Lyons, J. R., & Young, E. D. 2005, *Nature*, 435, 317, doi: [10.1038/nature03557](https://doi.org/10.1038/nature03557)
- Marrocchi, Y., Villeneuve, J., Batanova, V., Piani, L., & Jacquet, E. 2018, *Earth and Planetary Science Letters*, 496, 132, doi: [10.1016/j.epsl.2018.05.042](https://doi.org/10.1016/j.epsl.2018.05.042)
- McKeegan, K. D., Kallio, A. P. A., Heber, V. S., et al. 2011, *Science*, 332, 1528, doi: [10.1126/science.1204636](https://doi.org/10.1126/science.1204636)
- Menu, J., van Boekel, R., Henning, T., et al. 2014, *A&A*, 564, A93, doi: [10.1051/0004-6361/201322961](https://doi.org/10.1051/0004-6361/201322961)
- Morizet, Y., Paris, M., Gaillard, F., & Scaillet, B. 2010, *Chemical Geology*, 279, 1, doi: [10.1016/j.chemgeo.2010.09.011](https://doi.org/10.1016/j.chemgeo.2010.09.011)
- Nagahara, H., & Ozawa, K. 2012, *M&PS*, 47, 1209, doi: [10.1111/j.1945-5100.2012.01377.x](https://doi.org/10.1111/j.1945-5100.2012.01377.x)
- Nakamura, T., Noguchi, T., Tsuchiyama, A., et al. 2008, *Science*, 321, 1664, doi: [10.1126/science.1160995](https://doi.org/10.1126/science.1160995)
- Nomura, H., Furuya, K., Cordiner, M. A., et al. 2023, in *Astronomical Society of the Pacific Conference Series*, Vol. 534, *Protostars and Planets VII*, ed. S. Inutsuka, Y. Aikawa, T. Muto, K. Tomida, & M. Tamura, 1075
- Okamoto, T., & Ida, S. 2022, *ApJ*, 928, 171, doi: [10.3847/1538-4357/ac4bc1](https://doi.org/10.3847/1538-4357/ac4bc1)
- Olofsson, J., Augereau, J. C., van Dishoeck, E. F., et al. 2009, *A&A*, 507, 327, doi: [10.1051/0004-6361/200912062](https://doi.org/10.1051/0004-6361/200912062)
- Pérez, L. M., Chandler, C. J., Isella, A., et al. 2015, *ApJ*, 813, 41, doi: [10.1088/0004-637X/813/1/41](https://doi.org/10.1088/0004-637X/813/1/41)
- Sakamoto, N., Seto, Y., Itoh, S., et al. 2007, *Science*, 317, 231, doi: [10.1126/science.1142021](https://doi.org/10.1126/science.1142021)
- Schrader, D. L., Connolly, H. C., Lauretta, D. S., et al. 2013, *GeoCoA*, 101, 302, doi: [10.1016/j.gca.2012.09.045](https://doi.org/10.1016/j.gca.2012.09.045)
- Skorov, Y., Reshetnyk, V., Markkanen, J., et al. 2024, *MNRAS*, 527, 12268, doi: [10.1093/mnras/stad3994](https://doi.org/10.1093/mnras/stad3994)
- Tazaki, R., Ginski, C., & Dominik, C. 2023, *ApJL*, 944, L43, doi: [10.3847/2041-8213/acb824](https://doi.org/10.3847/2041-8213/acb824)
- Tazzari, M., Testi, L., Ercolano, B., et al. 2016, *A&A*, 588, A53, doi: [10.1051/0004-6361/201527423](https://doi.org/10.1051/0004-6361/201527423)
- Tenner, T. J., Ushikubo, T., Nakashima, D., et al. 2018, in *Chondrules: Records of Protoplanetary Disk Processes*, ed. S. S. Russell, J. Connolly, Harold C., & A. N. Krot, 196–246, doi: [10.1017/9781108284073.008](https://doi.org/10.1017/9781108284073.008)
- Ueda, T., Kataoka, A., Zhang, S., et al. 2021, *ApJ*, 913, 117, doi: [10.3847/1538-4357/abf7b8](https://doi.org/10.3847/1538-4357/abf7b8)
- Ushikubo, T., Kimura, M., Kita, N. T., & Valley, J. W. 2012, *GeoCoA*, 90, 242, doi: [10.1016/j.gca.2012.05.010](https://doi.org/10.1016/j.gca.2012.05.010)
- Weidenschilling, S. J. 1977, *MNRAS*, 180, 57, doi: [10.1093/mnras/180.2.57](https://doi.org/10.1093/mnras/180.2.57)
- Weidling, R., Güttler, C., Blum, J., & Brauer, F. 2009, *ApJ*, 696, 2036, doi: [10.1088/0004-637X/696/2/2036](https://doi.org/10.1088/0004-637X/696/2/2036)
- Yamamoto, D., Kawasaki, N., Tachibana, S., et al. 2024, *GeoCoA*, 374, 93, doi: [10.1016/j.gca.2024.04.014](https://doi.org/10.1016/j.gca.2024.04.014)
- Yamamoto, D., Kawasaki, N., Tachibana, S., Kamibayashi, M., & Yurimoto, H. 2022, *GeoCoA*, 336, 104, doi: [10.1016/j.gca.2022.09.006](https://doi.org/10.1016/j.gca.2022.09.006)
- Yamamoto, D., Kuroda, M., Tachibana, S., Sakamoto, N., & Yurimoto, H. 2018, *ApJ*, 865, 98, doi: [10.3847/1538-4357/aadcee](https://doi.org/10.3847/1538-4357/aadcee)
- Yamamoto, D., & Tachibana, S. 2018, *ACS Earth and Space Chemistry*, 2, 778, doi: [10.1021/acsearthspacechem.8b00047](https://doi.org/10.1021/acsearthspacechem.8b00047)
- Yamamoto, D., Tachibana, S., Kawasaki, N., & Yurimoto, H. 2020, *M&PS*, 55, 1281, doi: [10.1111/maps.13365](https://doi.org/10.1111/maps.13365)
- Yoshioka, T., Nakashima, D., Nakamura, T., Shehka, S., & Kepler, H. 2019, *GeoCoA*, 259, 129, doi: [10.1016/j.gca.2019.06.007](https://doi.org/10.1016/j.gca.2019.06.007)
- Yurimoto, H., & Kuramoto, K. 2004, *Science*, 305, 1763, doi: [10.1126/science.1100989](https://doi.org/10.1126/science.1100989)
- Zsom, A., Ormel, C. W., Güttler, C., Blum, J., & Dullemond, C. P. 2010, *A&A*, 513, A57, doi: [10.1051/0004-6361/200912976](https://doi.org/10.1051/0004-6361/200912976)